



ELSEVIER

Contents lists available at ScienceDirect

Journal of Non-Crystalline Solids

journal homepage: www.elsevier.com/locate/jnoncrysolKinetics of photo-dissolution within Ag/As₂S₃ heterostructurePritam Khan^{a,b,c}, Yinsheng Xu^b, William Leon^d, K.V. Adarsh^c, Dmitri Vezenov^d, Ivan Biaggio^e, Himanshu Jain^{b,*}^a Department of Physics, Kyushu University, 744 Motoooka, Fukuoka 819-0395, Japan^b Department of Materials Science and Engineering, Lehigh University, Bethlehem 18015, PA, USA^c Department of Physics, IISER Bhopal, Bhopal Bypass Road, Bhauri, Bhopal 462066, Madhya Pradesh, India^d Department of Chemistry, Lehigh University, Bethlehem 18015, PA, USA^e Department of Physics, Lehigh University, Bethlehem 18015, PA, USA

ARTICLE INFO

Keywords:

Thin films
Photo-dissolution
Chalcogenides
Pump-probe
Spectroscopy

ABSTRACT

Chalcogenide glass – silver heterostructures are candidates for photoresist and diffractive optical applications. To optimize their processing, we report the kinetics of Ag photo-dissolution in As₂S₃ matrix using in-situ optical transmission/reflection measurements and real time atomic force microscopy (AFM) imaging under optical illumination. The results indicate that photo-dissolution occurs in three stages with the extent and kinetics of each stage depending strongly on Ag film thickness. By contrast, the photo-dissolution is found to be independent of As₂S₃ matrix thickness. The extent of three stages also depends strongly on the laser dose and can be reduced to two stages at higher laser fluence. A comparative study of two oppositely stacked sample configurations: As₂S₃/Ag/glass and Ag/As₂S₃/glass show that the heterostructures respond differently to light illumination. For the former, Ag dissolves completely into As₂S₃ matrix at a faster rate than for the latter case. The origin of this difference is established by energy dispersive X-ray spectroscopy and AFM measurements.

1. Introduction

Heterostructures built from multiple components often exhibit physical-chemical properties that are not feasible with either of the individual components [1,2]. Silver-chalcogenide glasses (ChG) bilayers, such as As₂S₃/Ag, are of particular interest for the formation of multilayer heterostructures because of their potential applications in optics and optoelectronics [3,4]. An immediate application could be the fabrication of Programmable Metallization Cell (PMC) memory devices. Their formation requires the dissolution of metallic Ag into ChG matrix. Recently, Kozicki et al. [5] have shown that a solid electrolyte can be formed when 33 atomic % Ag is dissolved in Ge₃₀Se₇₀ [6]. Furthermore, the high transparency of ChGs in the IR region in combination with a variety of photo-induced effects can be used for making optical devices [6,7]. For example, in As₂S₃/Ag bilayer, photo-induced dissolution of metal Ag has attracted much interest for fabricating IR diffractive elements because it produces large changes in the physical and optical properties of glass, particularly its refractive index and etch resistance [8]. The dependence of dissolution rate on optical illumination renders these materials suitable for photoresists for lithography [9]. Upon irradiation with bandgap light, Ag and As₂S₃ layers start interacting with each other, changing the chemical composition as well as the structure

of the irradiated region compared to the unirradiated region [9]. Such photo-induced effects from the photo generation of electron-hole pairs alter the transmission, reflection, and micro-hardness of the heterostructure. Due to the difference in electron and hole mobility, holes diffuse away from the illuminated region faster than the electrons [10,11]. As a result, the negatively charged illuminated region attracts metal ions from the surface, complementing ion diffusion with a strong drift component [12]. However, the details of the underlying processes remain unclear. An understanding of the kinetics of Ag photo-dissolution in As₂S₃ can help us in optimizing the performance of these materials for photoresist and other applications.

Since the discovery of photo-dissolution by Kostyushin et al. [13], the time dependence of physical properties such as optical transmittance/reflectance [14] or electrical resistivity [15], and the concentration profile of Ag, have been determined [16]. Although a detailed explanation of the dissolution phenomenon is still being debated, it is generally believed that Ag photo-dissolution consists of three stages: (a) an induction period; (b) the effective photo-dissolution, and (c) a final stage that completes the photo-dissolution [16,17]. For practical applications, it is important to delineate these stages and also establish how they may be affected by the stacking sequence of these layers, especially in the context of multilayer structures. Accordingly,

* Corresponding author.

E-mail address: h.jain@lehigh.edu (H. Jain).<https://doi.org/10.1016/j.jnoncrysol.2018.09.001>

Received 9 August 2018; Received in revised form 30 August 2018; Accepted 1 September 2018

0022-3093/© 2018 Elsevier B.V. All rights reserved.

we have studied the kinetics of photo-dissolution in two oppositely stacked heterostructures of Ag and As_2S_3 films: $\text{As}_2\text{S}_3/\text{Ag}/\text{glass}$ and $\text{Ag}/\text{As}_2\text{S}_3/\text{glass}$ (from top to bottom). We have chosen As_2S_3 as the ChG matrix layer because sulfides have a higher ionic activity, which is favorable for investigating photo-dissolution mechanisms as well as practical applications. To obtain insights of the photo-dissolution process, we have varied the thickness of both Ag and As_2S_3 layers in either configuration. We have also performed real time atomic force microscopy (AFM) imaging under simultaneous optical illumination to obtain direct evidence of the photo-dissolution process at the nanoscale.

2. Experimental

Bilayer films of As_2S_3 ChG matrix and metallic Ag were deposited on a microscopy glass slide by conventional thermal evaporation in a vacuum of 1×10^{-6} mbar using commercially available bulk materials (5 N purity). A low deposition rate of 5–8 Å/s was maintained and continuously monitored using a quartz crystal. It is well known that such a low deposition rate produces thin films of composition that is very close to the starting bulk materials [18–21]. We prepared bilayer films in two different stacking configurations: $\text{As}_2\text{S}_3/\text{Ag}/\text{glass}$ and $\text{Ag}/\text{As}_2\text{S}_3/\text{glass}$ as shown in Fig. 1, where the absorption coefficient of As_2S_3 is $4.2 \times 10^3 \text{ cm}^{-1}$. We prepared three sets of samples: (1) with varying thickness of Ag layer (5, 10, 20 and 40 nm) for a fixed thickness of a- As_2S_3 matrix (Set 1), (2) with varying thickness of As_2S_3 matrix (430 and 860 nm) with fixed Ag layer thickness (Set 2), and (3) with opposite stacking sequence, where Ag is deposited at the bottom or the top of a- As_2S_3 (Set 3). The three sets of samples are listed in Table 1. The optical band gap (E_g) of all samples was calculated using classical Tauc plot [22]. We found that E_g varies between 2.38 eV (521 nm) to 2.40 eV (516 nm) for the samples used in the present study. Therefore, 488 nm (2.54 eV) laser provided near bandgap irradiation to the samples. We have used computer program “PARAV” for calculating the refractive index of all samples from experimentally measured transmission spectra of thin films [23]. The refractive index values of samples are shown in Table 1.

We have employed in-situ pump-probe optical transmission/reflection measurements. The bilayer is illuminated with a continuous wave 488 nm Ar^+ laser as pump beam with 4 mm spot size of intensity $7.5 \text{ mW}/\text{cm}^2$, and a very weak white light beam (400 to 900 nm) as probe with a very low intensity and a smaller diameter of 2 mm. The two beams are directed in such a way that they cross each other on the sample surface. The transmission/reflection through/from the sample is then measured by detecting the transmitted or reflected white light probe with a fiber optic Ocean Optics spectrometer, which has the ability to collect the entire spectrum in 2 ms. A schematic of the experimental set up is shown in Fig. S1 of Supplemental Information (SI). Note that for all measurements, the pump beam illuminated the top surface of the film. To assess the influence of light intensity on dissolution, the intensity of the pump beam is varied from 7.5 to 0.5 mW/

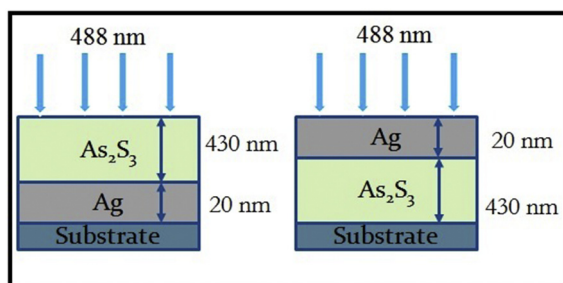


Fig. 1. Schematics of the heterostructure in two different geometric configurations: $\text{As}_2\text{S}_3/\text{Ag}/\text{glass}$ and $\text{Ag}/\text{As}_2\text{S}_3/\text{glass}$. The blue arrows show the direction of laser illumination. (For interpretation of the references to colour in this figure legend, the reader is referred to the web version of this article.)

Table 1

Different Sets of samples to study of Ag photo dissolution within As_2S_3 matrix. Set 1: Ag thickness is varied and is deposited below As_2S_3 of fixed thickness 430 nm. Set 2: 20 nm Ag is deposited below As_2S_3 whose thickness is kept at 430 and 860 nm. Set 3: Combination of Set 1 and 2, where 20 nm Ag is deposited top and bottom of 430 and 860 nm As_2S_3 .

Ag (nm)	As_2S_3 (nm)	Ag (position)	Set	Bandgap (eV)	Refractive index
5			Set 1	2.40 ± 0.002	2.38
10	430	Bottom		2.40 ± 0.003	2.42
20				2.39 ± 0.002	2.46
40				2.38 ± 0.001	2.56
20	430	Bottom	Set 2	2.39 ± 0.002	2.46
	860			2.38 ± 0.003	2.68
20	430	Bottom	Set 3	2.39 ± 0.002	2.46
		Top		2.38 ± 0.001	2.66
20	860	Bottom	Set 3	2.38 ± 0.003	2.68
		Top		2.38 ± 0.002	2.78

cm^2 . It is noteworthy that all the pump-probe measurements were performed under ambient condition.

AFM imaging was performed using an Asylum Research MFP-3D Bio atomic force microscope paired with an Olympus IX-71 inverted optical microscope. Illumination was provided by an X-Cite Series 120 broad-band light source filtered with an Olympus Z473/10 \times excitation filter (peak intensity 477 nm, FWHM 10 nm) and focused onto the sample plane with a 10 \times objective. The sample in this setup was illuminated from below and AFM imaging done from above. Power density in the sample plane during imaging was $1.4 \text{ mW}/\text{cm}^2$. Topographic images in air were obtained using a Budget Sensors Tap300Al cantilever in AC mode. Image scan size was set to $1 \mu\text{m} \times 1 \mu\text{m}$ (at 256×256 pixels) and taken at a scan rate of 2.1 Hz (requiring 121 s per image frame). The EDAX measurements were performed using Oxford INCA system with an X-Max detector.

3. Results and discussions

3.1. Photo-induced optical changes

To extract the contributions of individual layers, we measured the optical transmittance (T) of a pure Ag film and a pure a- As_2S_3 on a glass slide, and compared them with that of the bilayer heterostructure, as shown in Fig. 2a. Note that in the as-prepared state before the pump beam is switched on ($t = 0$) the transmission spectra of the bilayer are a composite of contributions from pure Ag and a- As_2S_3 , leading to a typical modulation in transmission that is caused by the interference of multiple reflections at the interfaces. These interference fringes contain a wealth of information about the structure of the deposited films and how they evolve in time. Notably, the bilayer spectrum exhibits similar interference fringes like a- As_2S_3 but modulated by the envelope (maxima/minima) of the transmission spectrum of pure Ag. With time the modulation part gradually diminishes, so that at the final stage of light illumination, the spectrum looks qualitatively similar to that of the pure As_2S_3 spectrum, except that it has shifted significantly to longer wavelengths. This evolution of the transmission spectra indicates that eventually Ag completely dissolves into the matrix and results in an optically homogeneous a-(Ag + As_2S_3) film.

To identify the stages of photo-dissolution, the transmission spectrum of the bilayer was recorded continuously in the presence of the pump beam illumination. A typical transmission curve is shown in Fig. 2b as a function of exposure time for one of the samples. The small spike at 488 nm is scattered light from the pump beam. The transmission spectrum is characterized by strong absorption edge followed by weekly absorbing interference fringes at longer wavelengths. To consistently quantify the results and correlate with the kinetics of photo-dissolution, we have focused on the second minimum of the transmission spectra after the absorption edge. The time-evolution of this

Download English Version:

<https://daneshyari.com/en/article/10155578>

Download Persian Version:

<https://daneshyari.com/article/10155578>

[Daneshyari.com](https://daneshyari.com)